MECHANISM AND SIMULATION OF THE MICROCRACKING PROCESS LEADING TO FRACTURE DURING LOW CYCLE FATIGUE

T. Magnin*, A. Bataille*, C. Ramade**

Two numerical modellings have been conducted to simulate the evolution during low cycle fatigue of a population of randomly nucleated surface microcracks in a 316L stainless steel. The aim of these modellings is to quantify the low cycle fatigue damage as a function of the evolution of the cracking processes. The cracking mechanisms are reviewed and introduced in the numerical simulations. The microcracks evolve in a statistic manner for their density and length distribution. An approach of the transition from low to high cycle fatigue is then possible with the simulations.

INTRODUCTION

During low cycle fatigue (LCF) at imposed plastic strain ($\Delta\varepsilon_p/2$) a considerable evolution of the surface roughness is experimentally observed in single phased polycrystalline materials. This evolution mainly corresponds to an early initiation and to the growth of a large number of microcracks (until 80 mm^{-2}) before a main crack can propagate through the bulk of the specimen, inducing fracture. In this paper, the micromechanisms of the microcracking process are described and numerical simulations of the related damage are proposed. Experiments have been performed mainly on austenitic 316L stainless steel cycled in tension-compression at imposed $\Delta\varepsilon_p/2$ in the range 4.10^{-4} to 4.10^{-3}. The scanning electron microscopy and the replica technics are used to study the evolution of the surface roughness.

MECHANISMS OF THE MICROCRACKING PROCESS

The exposed microcracking process is related to fcc 316L and can be described in several stages. The first stage occurs at the scale of the grain. The cyclic deformation localizes in intense slip bands along which the first transgranular microcracks appear (1). Those surface micro-

* Université de Lille 1, Villeneuve d'Ascq Cedex
** Ecole des Mines, Saint-Etienne, France

cracks correspond to the so called type I microcracks with a surface length L lower than 50 µm (average grain size in the austenitic steel). They develop by cristallographic micropropagation. Some of type I microcracks grow crystallographically accross one or two grain boundaries and lead to type II microcracks with 50<L<150 µm (stage II). Stage III corresponds to the microcoalescence between type I and type II microcracks which induces the formation of type III microcracks with 50<L<500 µm. They are perpendicular to the mean stress axis. The last stage includes surface propagation and coalescence of some of those microcracks and leads to the formation of one or two type IV cracks which propagate through the bulk of the specimen and induce fracture (2).

Figure 1 shows an example of the evolution of each kind of microcracks for the plastic strain amplitude $\Delta\varepsilon_p/2 = 2.10^{-3}$. Note that N_i corresponds to the number of cycles for the recording of a 1 % rapid decrease of the peak stress level. Relating to the evolution of those different types of microcracks, Magnin et al (1) reported a similar behaviour for bcc and fcc single phased polycrystals (with a plastic strain amplitude of 2.10^{-3}) when using the number of cycles reduced to N_i (figure 2). Type I microcracks seem to appear approximately at 0.1 N_i, type II at 0.2/0.3 N_i and type III for 0.5 N_i.

Then describing the fatigue damage with the statistic evolution of a population of surface microcracks seems to be of great interest. Two different numerical modellings of the fatigue damage with transgranular microcracking have been conducted.

FIRST NUMERICAL MODELLING

The mesh is made of squares which represent the grains. The computation nucleates only one microcrack per grain. The tested area regroups 3770 squares or grains. Microcracks are nucleated randomly. They are classified in three types according to their lengths and to their typical growth behaviour.

Those new types regroup different microcrack types defined above, depending on the stress level. In other words, type A corresponds to type I microcracks, but types B and C are defined from the empirical relation $\sigma_s . \sqrt{L_t} = 2.7$ MPa.m$^{1/2}$ (where σ_s is the peak stress level). This relation leads to calculate a threshold length L_t (3). Type C microcracks correspond to microcracks the length of which is longer than L_t. The type B one regroup the microcracks with a length in the range 50 to L_t µm.

Type A microcracks grow linearly cycle after cycle till the grain boundaries. Then they become type B microcracks. Those cracks only grow crystallographically when another crack tip exists at a distance lower than two grain sizes. When two microcracks reach the same square, they can coalesce. The type C microcracks grow with the empirical law $L_N = (1+y).L_{N-1}$ (a geometrical progression) where N is the number of

cycles and y is a parameter depending on the material and on the plastic strain amplitude (3). They are able to coalesce with other microcracks the tips of which are in the closed tip squares. The microcracks just grow perpendicularly to the main stress axis. The software consists in nucleation, propagation (when it is possible) and coalescence for all the microcracks, the one after the other.

When all the microcracks are tested, the number of cycles N increases of one unit. The computation ends when the greater crack is 2000 µm, at $N = N_i$. Figure 3 presents the results for a plastic strain amplitude of $\Delta\varepsilon_p/2 = 4.10^{-3}$. A good agreement with the experimental results is observed.

SECOND NUMERICAL MODELLING

This new modelling include two new features, the grain shape and the grain orientation. The grains are represented by hexagons which are divided in 36 squares. The entire mesh contains approximately 300 grains and then simulates a computation area somewhat like 2/3 mm^2. The software includes a nucleation of microcracks, their propagation and their coalescence at the specimen surface.

About the nucleation

For each undamaged square, a random number is generated in the range 0 to 1. When this number is higher than the nucleation threshold defined by the operator, the square is cracking. This threshold is depending on the plastic strain amplitude. It is more and more closed to the unit when the strain amplitude decreases.

About the propagation

The nucleated microcracks propagate through the grains from square to square. To have cracking of the square closed to the crack tip one's, the software computes a random number. If it is higher than the propagation threshold, then the square is cracking. The propagation threshold is calculated from the nucleation threshold. It decreases when the number of unsuccessful cracking tests increases.

In the other hand, the propagation threshold increases with the misfit between the easy cracking direction of the crack tip square and the easy cracking direction of the tested one.

About the coalescence

During the computation, the microcrack coalescence process occurs. The criterion of coalescence between two closely spaced microcrack tips has been chosen from the paper of Ochi et al (4) who worked on the fcc 304 stainless steel. The coalescence of two closely cracks in this steel is possible when the distance between the tips is lower than

11 % of the two lengths addition. In fact, the coalescence really occurs with the formation of types II and even III microcracks. The software then consists in testing each undamaged square for nucleation, propagation and coalescence. A screen display makes easier the follow up of the microcracks evolution. The computation ends when the greater microcrack reaches then the length of 50 closed squares (approximately 350 to 400 μm).

Figure 4 shows an example of the results in the case of a plastic strain amplitude $\Delta\varepsilon_p/2 = 4.10^{-3}$. A good agreement with the experimental results is observed.

CONCLUSION

The two computations are in good agreement with the experimental results for the relatively high plastic strain amplitude $\Delta\varepsilon_p/2 = 4.10^{-3}$ (when expressing with the reduced number of cycles for the second modelling).

Two different empirical relations occur in the first modelling while the new one works only with random probability laws. Those empirical relations lead to ungrowing periods and other periods with increasing growth rate, concerning the type B microcracks. The new modelling also includes this kind of behaviour which has been observed by Ramade (3) and Polak (5). This means merely that to quantify the low cycle fatigue, we have to treat a population of microcracks in a statistical way.

The agreement between computed and experimental results is not so good when the softwares are used for high cycle fatigue damage. The reason must be found in the relatively smaller microcrack density at low $\Delta\varepsilon_p/2$. Then the microcoalescence processes occur less frequently and the formation of long surface microcracks is delayed. Moreover, the ratio between surface propagation and bulk propagation evolves to the benefit of the bulk propagation.

The future purpose of numerical modellings will be to determine the range of plastic strain amplitude, which corresponds to the shift of surface cracking to bulk cracking processes in the fcc 316L stainless steel. The new software will also include several modules to have more flexibility for studying the effects of shape (morphological texture), of grain orientation (crystallographical texture) and of cumulative damage.

REFERENCES

(1) Magnin, T., Ramade, C., Lepinoux, J. and Kubin, L.P., Mater. Sc. Engng. A118, 1989, pp.41-51.

(2) Magnin, T., Coudreuse, L. and Lardon, J.M., Scripta Metallurgica, Vol. 19, 1985, pp.1487-1490.

(3) Ramade, C., Thesis, St Etienne, 1990.

(4) Ochi, Y., Ishii, A. and Sasaki, Y.K., Fatigue Fract. Engng. Mater. Struc., Vol. 8, 1985, pp.327-339.

(5) Polak, J. and Liskutin, P., Fatigue Frac. Engng. Mater. Struc., Vol. 9, 1990, pp.119-133.

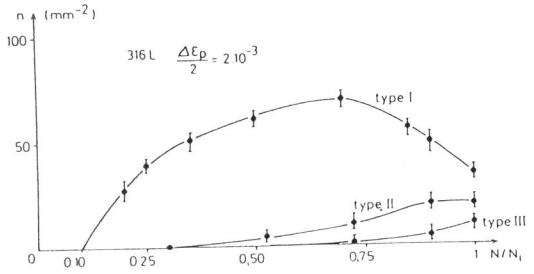

Figure 1 Experimental evolution of each kind of cracks in 316L alloy $\Delta\varepsilon_p/2 = 2.10^{-3}$

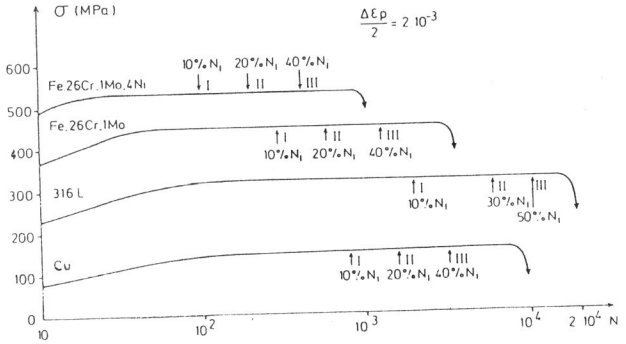

Figure 2 Experimental evolutions of each kind of cracks in different materials $\Delta\varepsilon_p/2 = 2.10^{-3}$

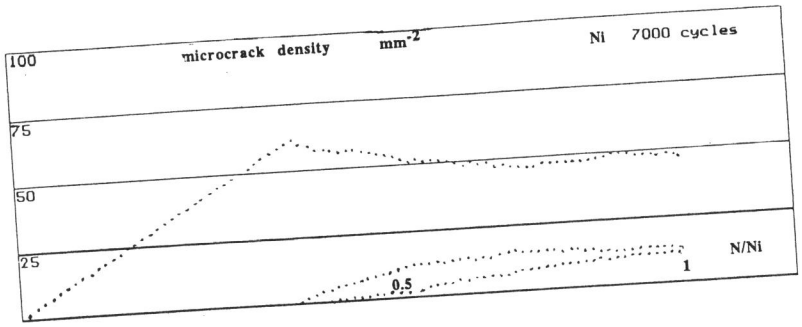

Figure 3 Evolution of the crack populations in the first modelling for $\Delta\varepsilon_p/2 = 4.10^{-3}$

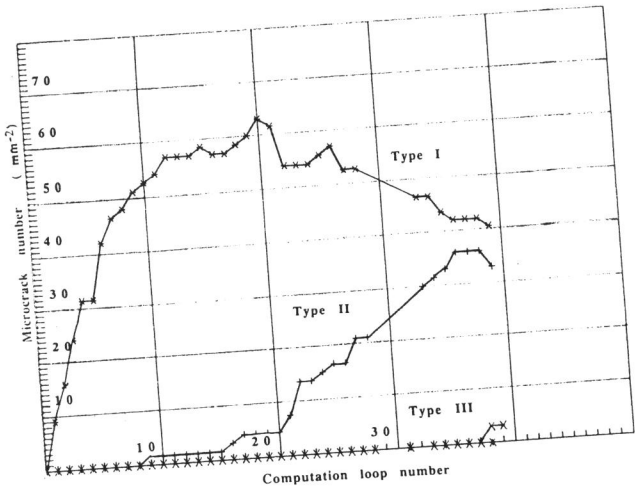

Figure 4 Evolution of crack populations in the new modelling for $\Delta\varepsilon_p/2 = 4.10^{-3}$